7th International Symposium on Superalloy 718 and Derivatives
Edited by: E.A. Ott, J.R. Groh, A. Banik, I. Dempster, T.P. Gabb, R. Helmink, X. Liu, A. Mitchell, G.P. Sjöberg, and A. Wusatowska-Sarnek
TMS (The Minerals, Metals & Materials Society), 2010

CONSIDERING THE SOLIDIFICATION STRUCTURE OF VAR INGOTS IN THE NUMERICAL SIMULATION OF THE COGGING PROCESS

Jan Terhaar[1], Jörg Poppenhäger[1], Dieter Bokelmann[1], Hendrik Schafstall[2], Kanchan Kelkar[3]

[1]Saarschmiede GmbH Freiformschmiede; Bismarckstraße 57-59, 66333 Völklingen, Germany
[2]simufact engineering GmbH; Tempowerkring 3, 21079 Hamburg, Germany
[3]Innovative Research, Inc.; 3025 Harbor Lane N, Suite 300, Plymouth, MN 55447, USA

Keywords: VAR, Solidification Texture, Anisotropic Yield, Damage Behavior, Forging, Numerical Simulation, Alloy 718

Abstract

The main objective of Vacuum Arc Remelting is to control solidification conditions in order to obtain a columnar dendritic structure throughout the whole ingot. The change in primary dendrites' growth direction, determined by the pool shape, leads to non-isotropic material properties in terms of plastic flow. As the correct prediction of flow behavior is crucial for the further analysis of forming processes (as for example in the application of damage criteria), this specific feature of remelted material has to be accounted for in the modeling of ingot breakdown. Using Barlat's formulation for the plastic flow, the structural constitution of alloy 718 VAR ingots could be linked to the alloy's plastic flow behavior by modeling the inhomogeneity of properties determined by remelting experiments and simulations. Hence, the influence of different remelting process conditions on hot workability could be examined. Compared to the commonly used von Mises approach some differences could be revealed.

Introduction

It is unquestionable that solidification conditions affect different aspects of the material's behavior during subsequent forging operations. On the one hand the plastic yield is influenced directly by crystal orientations, on the other hand the amount of segregation can have a strong impact on the workpiece's resistance to damage. In remelting processes both features are closely related to the pool profile of the growing ingot, which in turn is governed by the process conditions. While the shape of the molten pool determines the primary dendrites' growth direction, i.e. the distribution of solidification angles with respect the longitudinal axis of the ingot, the pool depth is responsible for the local solidification time, i.e. the resulting degree of segregation depending on the radial position within the ingot. Since these aspects are considered to be relevant and influential for the material's behavior in terms of plastic yield and damage evolution during primary forging steps, they have to be accounted for in the numerical simulation, when the results are expected to give a realistic representation of the observed material behavior. However, possible influences from preceding processes are usually neglected in the simulation. In order to reduce the modeling efforts, the material properties commonly used in the finite element simulation of forming processes are assumed to be isotropic and homogeneous, which actually is not the case when considering the as-cast or homogenized state.
Hence, the intention of this work was to develop a material model capable of considering the mentioned aspects regarding the solidification structure of vacuum arc remelted ingots in the numerical simulation of forging operations, as for example cogging.

Anisotropic Yield

The preferred orientation in the solidification of face-centered cubic (fcc) metals such as alloy 718 is aligned to the crystallographic [100] direction, leading to a certain solidification texture in remelted superalloy ingots [1]. Consequently, the (111) slip planes, mainly responsible for the plastic yield behavior, are not arbitrarily oriented either, leading to anisotropic deformation.
Investigations concerning the hot rolling of directionally solidified and hence texturized material, revealed that the required rolling forces were depending on the orientation of the dendrites' axes with respect to the rolling direction [2]. Remarkably, the differences in rolling forces were still present after several passes and significant reduction, indicating that despite recrystallization the effect of a solidification texture is quite persistent. Although it has been shown in several publications that the solidification texture of remelted material results in anisotropic yield, it has not been attempted to account for it in the numerical analysis of hot working processes. By conducting upsetting tests to determine flow curves for the as-cast or homogenized state, other authors have noticed the 'strange' deformation behavior without further analyzing it [3,4]. Regarding the upsetting of cylindrical specimens this expresses in elliptical barreling.

Damage Behavior

When evaluating the damage behavior of a material, it is a common approach to first conduct upsetting tests and detect the occurrence of cracks. After a forming limit has been determined in these experiments, the upsetting is simulated in order to identify the values of damage criteria, present at the spot, where the experiment had shown the cracks to originate [5]. However, this is only possible, when plastic flow is predicted correctly. The fact, that it is not possible to account for the non-isotropic deformation of texturized cast structures with the commonly applied von Mises yield criterion gave reason to look for an anisotropic material law that could be expanded to the use under hot working conditions. Furthermore, the susceptibility of a material to damage nucleation strongly depends on its microstructural condition. When a superalloy ingot is subjected to its first deformation during ingot breakdown, it has passed two processes significantly influencing its hot working properties, solidification and homogenization. In terms of alloy 718 the duration of solidification controls the amount and distribution of Laves phase [6]. The dissolution of this deleterious phase is depending on the way the homogenization treatment is carried out [7,8]. Consequently, the workpiece's resistance to damage can only be linked directly to the solidification conditions, if the same homogenization treatment is applied.

Experimental and Numerical Procedure

The procedure in this investigation covers both, an experimental part to reveal real material behavior and a numerical part to represent the observed behavior in the numerical simulation. It can be structured in the following steps:

- examination of real material behavior in the as-cast and homogenized state,
- simulation of the remelting process,
- identification of relevant features of the cast structure,
- conversion of remelting simulation results into properties of the workpiece,
- calibration of the material model with respect to plastic yield and damage evolution and
- simulation of the cogging process using the adapted material model.

In order to analyze the real material behavior in terms of plastic flow and damage evolution, a series of upsetting tests with large sized cylindrical specimens (∅55.6 × 100 mm) was carried out. These specimens were taken from several ∅504 mm alloy 718 VAR trial ingots and additionally from different radial positions of these ingots. Also, the radial direction of the ingot

was marked with two indentations on the front face of each specimen. To be able to cover different solidification conditions within these specimens, the mentioned batches were remelted with different helium gas cooling parameters while applying the same melt schedule. Prior to upsetting, these specimens were subjected to a reference homogenization treatment.
However, for a series of specimens from the same radial position of the same ingot, i.e. where the solidification conditions can be assumed roughly the same due to the rotational symmetry of the process, different homogenization treatments were applied. Furthermore, two different upset strains were realized with these specimens; 20% and 50% height reduction. All specimens were heated to an upsetting temperature of 1075°C in an electric furnace and after equalizing for ~ 1.5 h the specimens were upset on an industrial 10 MN hydraulic forging press to the predefined final height (80 mm or 50 mm, respectively). Afterwards they were quenched in water immediately. Some of the upset specimens are shown in Figure 1.

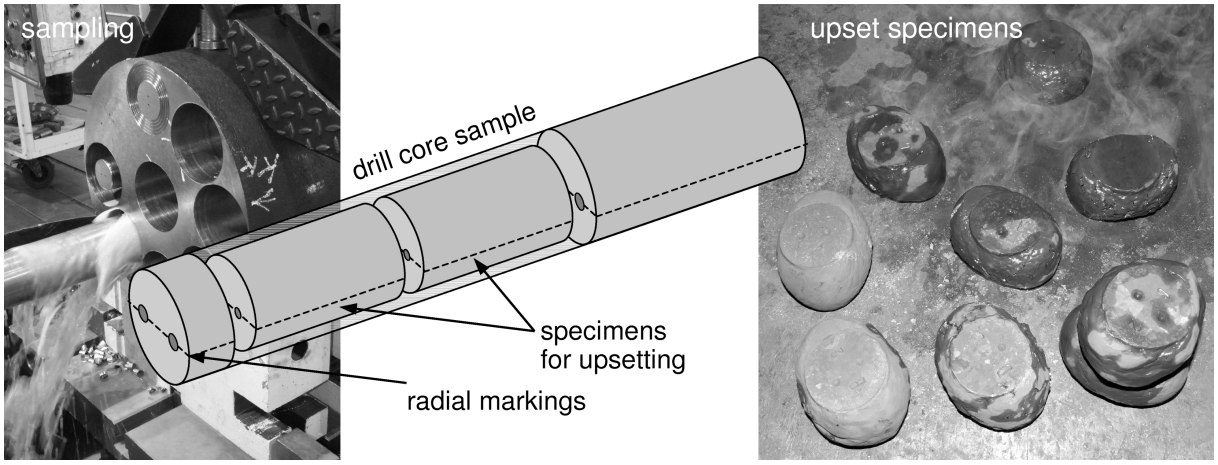

Figure 1. Sampling (left) and specimens after upsetting (right).

Regarding the influence of the directional solidification on plastic flow behavior, it could clearly be shown that the solidification texture results in elliptical barreling of the specimens, with the barreling ellipse having a preferred orientation. In all specimens from the outer region of the ingot's cross-section, the maximum diameter of the elliptical shape was oriented perpendicular to the radial markings on the specimen's front face, i.e. aligned to the circumference. This could be observed regardless of the previously applied homogenization treatment. The diameter ratio d_{max}/d_{min} that acts as a measure for the extent of plastic anisotropy reached a value of 1.3 for the specimens close to the rim of the ingot and was steadily falling towards a value of 1.0 for the center position (representing the isotropic case).
Regarding the materials susceptibility to damage, it was obvious that homogenization practice has a strong influence. However, for a given homogenization treatment, a comparison of upset specimens from the different VAR batches suggested that solidification conditions affect the damage behavior in that way, that a prolonged solidification time weakens the material's ability to withstand crack nucleation. The specimens from a batch with no helium cooling and hence a rather deep pool showed significant damage in contrast to the material from a batch with strong cooling and a quite shallow pool.

Simulation of Vacuum Arc Remelting

Any influence on the molten metal pool mirrors in the resulting microstructure of the as-cast material. Assuming that the directional solidification can be maintained throughout the entire cross-section of the ingot, the distribution of solidification angles, which is responsible for the anisotropic yield, can be directly influenced by altering the process conditions affecting the pool

profile. Simultaneously, the local solidification time and hence the segregation potential and dendrite arm spacings are altered as well, which in turn has a strong influence on the workability. To be able to find a link between the observed behavior of the upset specimen and certain properties of the solidification structure, the remelting processes (producing the ∅504 mm alloy 718 ingots that the samples were taken from) were simulated based on the real process data using the commercial software MeltFlow-VAR by Innovative Research. The required material data for the liquid metal was taken from literature [9], whereas the relation between helium cooling parameters and the appropriate boundary condition for the convective heat transfer in the gap between ingot and crucible was determined in previous work [10]. The simulation results for two batches with different helium cooling conditions (i.e. gas flow rates) are depicted in Figure 2. Due to confidentiality reasons there are no absolute values given in the trace of the melt rate.

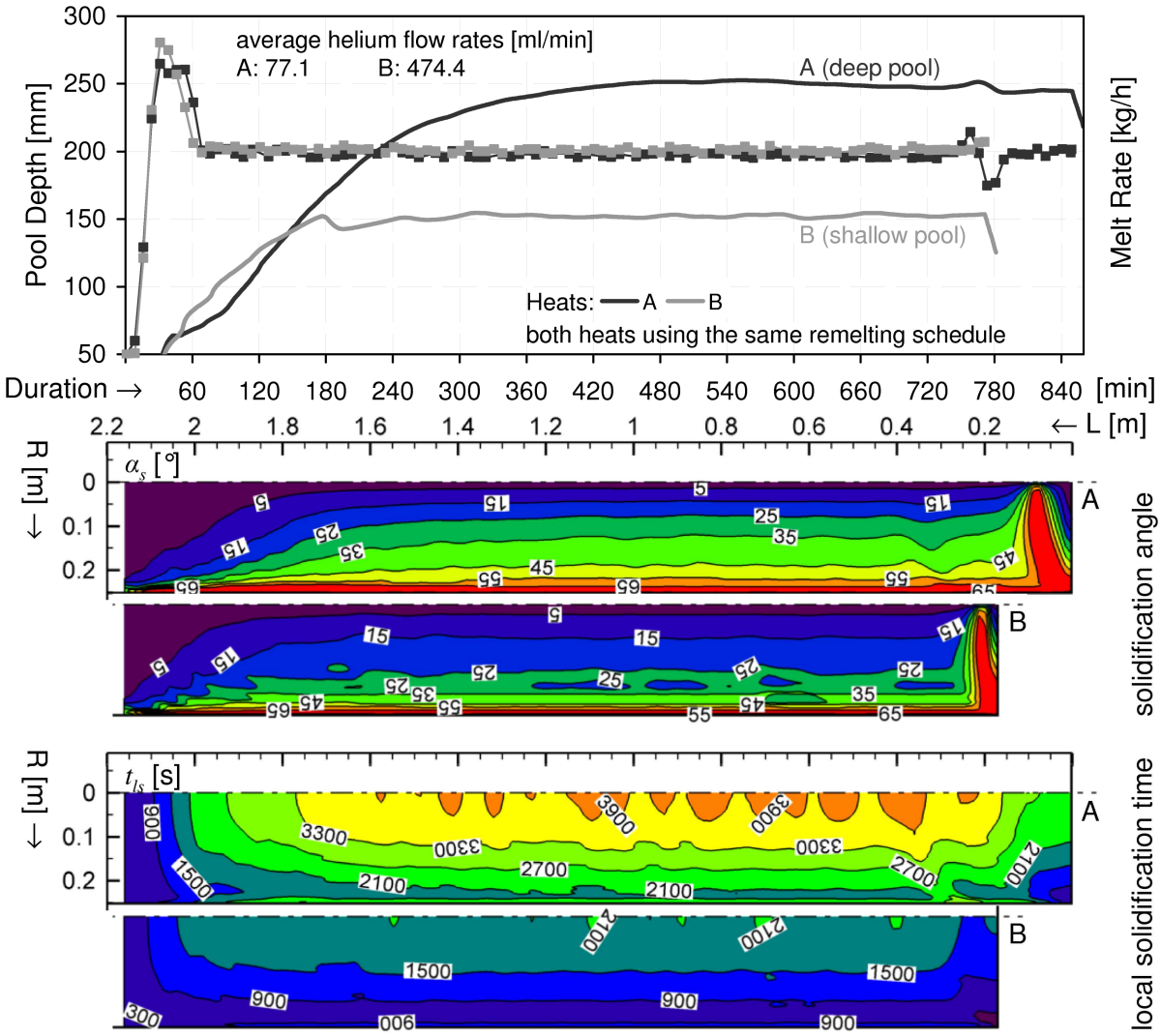

Figure 2. Simulation of VAR; specified process conditions (top) and results (bottom).

The distribution of solidification angles α_s derives from the development of the pool profile as a function of process duration, i.e. the slope of the contour line for a given solid fraction (here: $f_s = 0.9$) is evaluated continuously during remelting, so that the angle between the thermal gradient G (which equals the primary dendrites' growth direction) and the gravity vector can be interpreted as a property of the ingot's metallurgical structure.

The distribution of local solidification time t_{ls} simply represents the duration of passing the temperature range between liquidus and solidus. These two properties were considered to be the relevant factors for a realistic description of forming behavior of remelted material.

Transfer of Simulation Results

The conversion of VAR simulation results into additional material properties that can be accounted for in the numerical modeling of forging processes consists of two steps. First, the relevant quantities (like α_s and t_{ls}) have to be assigned to the finite elements of the model used in the forging simulation. Then second, the functional relations describing the connection between the material's metallurgical structure and its plastic properties have to be available.
To accomplish the first step, the geometrical data of the contour lines for α_s and t_{ls} were exported from the results and read into the preprocessor of the simulation tool simufact.formingSFM used for the forming analysis. By revolving these curves, iso-surfaces for both properties were created with the discretization according to Figure 2. By placing the finite element model of the cylindrical specimens at their position within the ingot these surfaces could then be used for element selection, as it is shown in Figure 3.

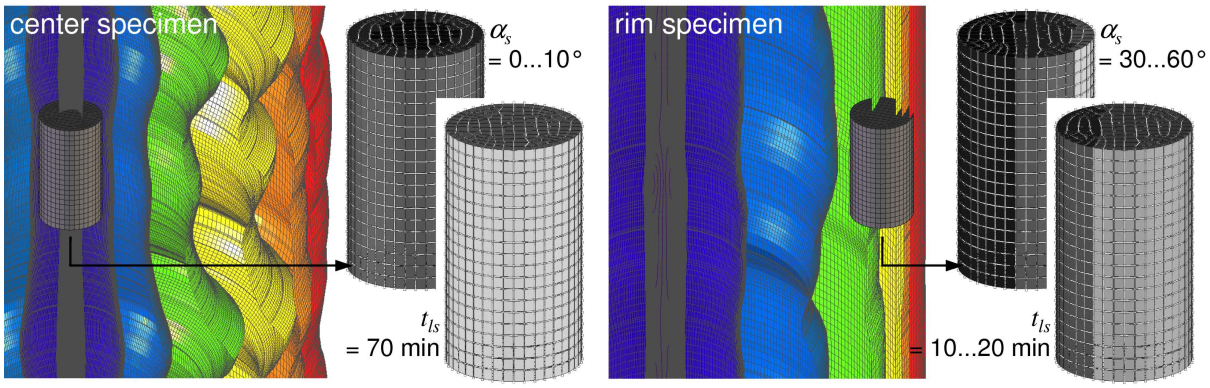

Figure 3. Transfer of simulation results.

In this way, each finite element of the model would obtain two additional properties directly related to the process conditions during remelting. In order to reveal the required relations

- anisotropic plastic yield as a function of the solidification angles α_s and
- critical damage values as a function of the local solidification time t_{ls},

the already presented upsetting tests were used for calibration purposes with the intention to reconcile the observed material behavior with the numerical simulation.

Simulation of Upset Forging

Since anisotropic material laws are usually used in the analysis of cold forming processes, an appropriate yield criterion had to be found that could be applied to hot working of bulk metal. Hence, simufact engineering created the possibility to use Barlat's yield criterion with hot working flow curves, so that besides the dependency of strain, strain rate and temperature the yield stress could also be scaled in different directions according to the orientation of the element coordinate system. The yield criterion is defined as [11]

$$f = |S_1 - S_2|^m + |S_2 - S_3|^m + |S_3 - S_1|^m = 2\,\sigma^m \qquad (1)$$

with $S_{i=1,2,3}$ representing the principal values of the symmetric matrix $S_{i,j}$ given as

$$S = \begin{bmatrix} \frac{C_3(\sigma_{xx}-\sigma_{yy})-C_2(\sigma_{zz}-\sigma_{xx})}{3} & C_6\sigma_{xy} & C_5\sigma_{zx} \\ C_6\sigma_{xy} & \frac{C_1(\sigma_{yy}-\sigma_{zz})-C_3(\sigma_{xx}-\sigma_{yy})}{3} & C_4\sigma_{zy} \\ C_5\sigma_{zx} & C_4\sigma_{zy} & \frac{C_2(\sigma_{zz}-\sigma_{xx})-C_1(\sigma_{yy}-\sigma_{zz})}{3} \end{bmatrix}. \quad (2)$$

The symmetry axes (x,y,z) define the axes of anisotropy, which originally are aligned to the initial rolling, transverse and normal direction (see Figure 4). The material coefficients $C_{i=1\ldots6}$ in Equation 2 govern the anisotropic properties. When the parameters are set $C_{i=1\ldots6} = 1$ and $m = 2$ (or 4) Equation 1 reduces to the von Mises yield criterion, so that the material becomes isotropic. Generally, an increase in the value of the exponent m, which is mainly associated to the alloy's crystal structure, leads to a decrease of the round vertices' curvature near the uniaxial and balanced tension ranges of the yield surface; for fcc materials like superalloys a value of $m = 8$ is recommended. Assuming further, that plastic yield properties in transverse directions are isotropic (C_4=C_5 = 1), there are four unknown independent coefficients remaining (C_1, C_2, C_3 and C_6). In the case of sheet metal forming these values can be calculated from experimental data regarding σ_0, σ_{45}, σ_{90} and σ_b, representing the tensile yield stresses at 0°, 45° and 90° from the rolling direction and the balanced biaxial stress, respectively [12]. In bulk metal forming where the flow stresses usually are measured in compression tests, these values are not readily available, so that they finally had to be fitted. Thus, the orientation dependency introduces a comparably large number of additional degrees of freedom into the modeling of a forging process, since the required parameters for the anisotropic yield criterion cannot simply be determined as in sheet metal forming. Consequently, in a rather phenomenological approach, the elliptical barreling of the upset specimens was used to calibrate the material law by simply finding the best fit between real and simulated behavior. Therefore a series of thermo-mechanically coupled simulations of the specimens' upsetting was carried out in order to find the best fit between the measured and the calculated diameter ratio d_{max}/d_{min}.

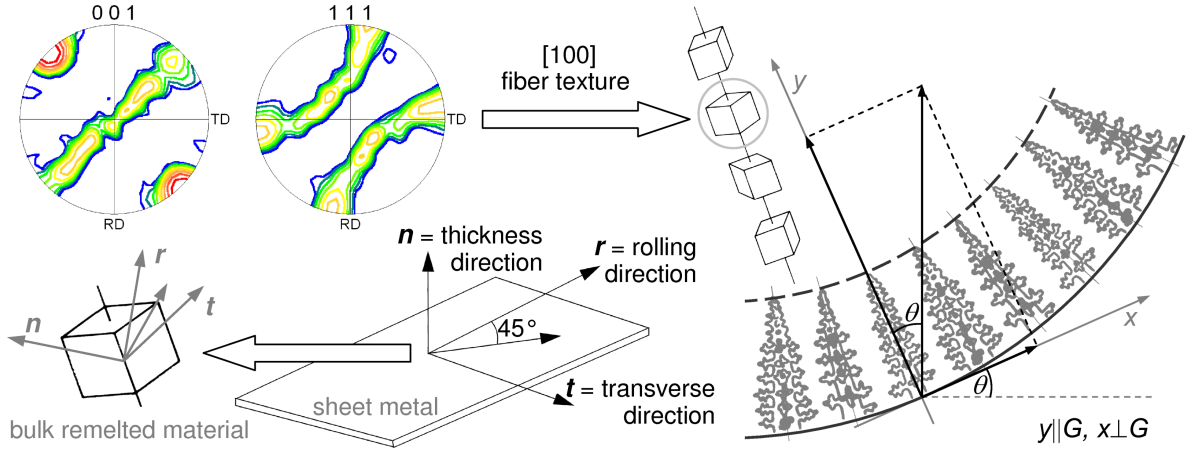

Figure 4. Modeling the anisotropic yield related to the preferred orientation in solidification.

However, not only the model parameters have to be determined but also an appropriate connection between the solidification angles and the finite element's coordinate system had to be found. This could be derived from an electron backscatter diffraction analysis, showing that the [100] fiber texture is accompanied by a preferred orientation of the (111) slip planes. Figure 4 shows the crystallographic orientation of the unit cells and the numerical interpretation by the finite elements' coordinate system.

With this link to the metallurgical structure of the ingot, each finite element was given a specific orientation according to the results predicted by the remelting simulation; a Python script automatically performed the elemental rotations. It turned out, that by orienting the elements' coordinate system in the way described, slightly raising the ratio σ_{45}/σ_0 produced the elliptical barreling that the practical upsetting tests had shown. Since the σ_{45}-direction equals the orientation of the normal vector to the octahedral planes in the three-dimensional model of the bulk metal forming process, it is quite unfavorably oriented to activate the main slip planes in contrast to σ_0 and σ_{90}. Thus, a raise of the yield stress in this direction is somewhat consistent with the results of the microstructural analysis presented in Figure 4. An overview of the calibration procedure is given in Figure 5.

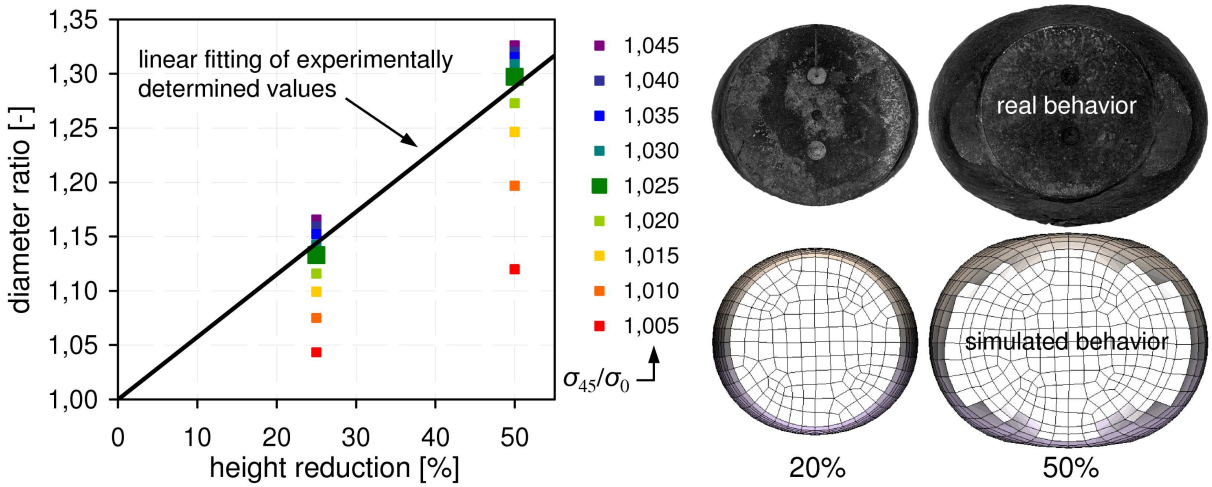

Figure 5. Calibration of the anisotropic material law.

The fitting curve represents the experimental measurements, whereas the colored points show the calculated dimensions of the barreling ellipse. As can be seen, the best agreement was achieved by scaling up the flow stress 2.5% in σ_{45}-direction, leading to the following set of coefficients for the yield criterion:

$$m = 8; \quad \sigma_{45}/\sigma_0 = 1.025,\ \sigma_{90}/\sigma_0 = \sigma_b/\sigma_0 = 1.0 \quad \rightarrow \quad C_{i=1\ldots5} = 1.0 \text{ and } C_{i=6} = 0.967157$$

Given the usual scattering of the flow stress in the as-cast or coarse-grained homogenized state, this scaling can be considered negligible. With this anisotropic material law using flow stress data for alloy 718 determined under usual hot working conditions ($\varphi \leq 1.0$, $d\varphi/dt = 0.01\ldots1.0\ s^{-1}$, $\vartheta = 875\ldots1125°C$), the observed material behavior could be modeled quite realistic. However, it has to be mentioned, that the plastic anisotropy could only be reproduced in the simulation by using a kinematic work hardening approach for the interpretation of the underlying flow curves.

The requirement of predicting the plastic flow correctly had to be fulfilled in a first step to determine critical values regarding the damage evolution in a second step. There are numerous damage criteria reported in the literature, out of which in the context of this work, two very popular ones were selected to find a correlation between the local solidification time and a critical damage value. The criterion by Cockcroft & Latham (C&L) [13] and a modified one also proposed by Le Roy et al. (LR) [13,14] defined as

$$D_{C\&L} = \int \max[\sigma_I, 0]\, d\bar{\varepsilon}^p \tag{3a}$$

$$D_{LR} = \int \left(\max[\sigma_I, 0] - \sigma_m\right) d\bar{\varepsilon}^p \qquad \text{where } \sigma_m = \left(\sigma_I + \sigma_{II} + \sigma_{III}\right)/3 \tag{3b}$$

were applied to the upsetting simulation and proved capable of localizing the spot of damage initiation. For the reference homogenization, it was observed that a specimen from the center

position of a VAR batch with no helium cooling and hence quite high values of t_{ls} predicted in the corresponding simulation showed first signs of peripheral cracking already at the lower height reduction of 20%. On the contrary, another specimen taken from the rim position of a batch with strong helium cooling and consequently characterized by a comparably low value of t_{ls} showed approximately the same extent of damage at the higher height reduction of 50%.
By determining the damage values for these two specimens according to the mentioned criteria at the location of crack initiation, i.e. in the equatorial plane on the lateral surface parallel to d_{max}, the susceptibility to damage could be considered in relation to the local solidification time.
As a result, the damage criteria given in Equations 3a and b could be transformed into an expression describing the probability of damage occurrence as a function of solidification conditions. This calibration procedure in terms of damage is shown in Figure 6.

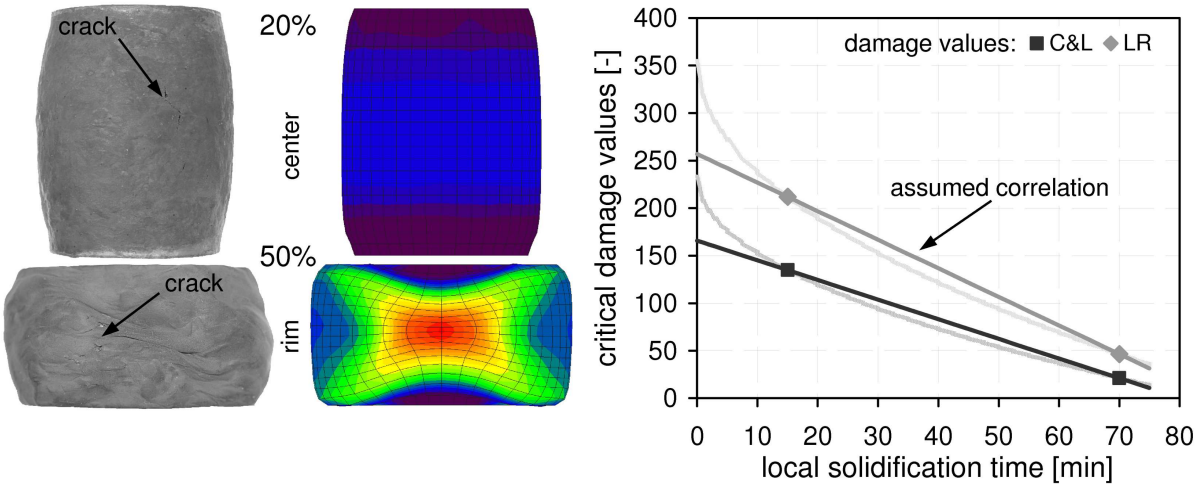

Figure 6. Calibration of the selected damage criteria.

The resulting normalized Cockcroft & Latham and Le Roy criteria for alloy 718 (heat treated with the reference homogenization) are calculated by

$$P_{C\&L} = \frac{D_{C\&L}}{D^*_{C\&L}(t_{ls})} = \frac{\int \max[\sigma_I, 0]\, d\bar{\varepsilon}^p}{a \cdot t_{ls} + b} \quad \text{with } a = -2.067795 \text{ and } b = 165.829578 \tag{4a}$$

$$P_{LR} = \frac{D_{LR}}{D^*_{LR}(t_{ls})} = \frac{\int (\max[\sigma_I, 0] - \sigma_m)\, d\bar{\varepsilon}^p}{a \cdot t_{ls} + b} \quad \text{with } a = -3.007242 \text{ and } b = 256.900236 \tag{4b}$$

where a linear relation between the average t_{ls} [in min] and the critical values $D^*_{C\&L}$ and D^*_{LR} is assumed (see Figure 6). Of course, due to the small number of specimens and the vague interpretation of actual damage initiation, this relation is just a rough estimation and only capable of representing a general tendency. For a more precise representation a larger number of upsetting tests would have to be evaluated with the possibility to detect damage initiation more accurately.
However, it has to be pointed out that these experiments cannot simply be carried out under laboratory conditions, since most testing machines used to perform compression tests are limited to smaller sample dimensions. However, the specimens have to cover a sufficient number of grains to allow for the microstructural weakness of the grain boundaries. Due to the fact, that a high temperature homogenization treatment results in a very coarse-grained structure (containing grains with diameters > 10 mm), the specimens have to be upsized correspondingly, as it was done in this investigation. Nevertheless, Figure 7 confirms that the damage behavior of the upset specimens can be described properly with this approach; color scale: violet (0.9) to red (1.0).

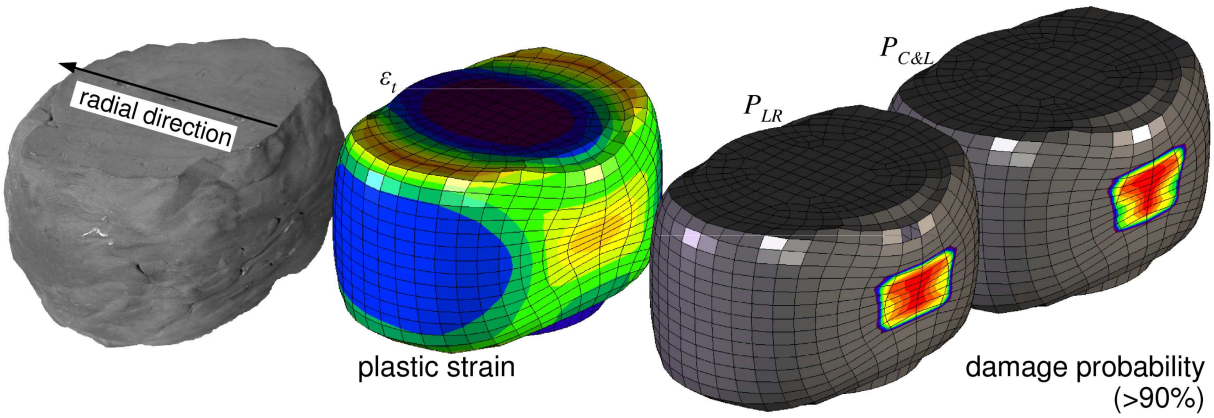

Figure 7. Comparison of real and simulated behavior with the adapted material model.

Cogging

The material law, calibrated in terms of anisotropic plastic yield and damage susceptibility for alloy 718 in the homogenized state, could finally be used to perform calculations of the cogging process. By transferring the mentioned features of the ingots' metallurgical structure into the forming simulation of ingot-to-billet conversion, the effect of helium cooling during VAR could be further evaluated. The two ingots (heat A: moderate helium cooling ⇒ comparably deep pool; heat B: intense cooling ⇒ shallow pool) were numerically subjected to the following pass schedule for cogging from ∅470 to ⍁370 [dimensions in mm] with bites of 360 mm using the classical 1|½|1|½-shift

		1st pass	90°	2nd pass	-90°	3rd pass	90°	4th pass
~470	→	390	→	400	→	350	→	370

In the numerical simulation of cogging, the initial forging temperature was set to 1100°C and in terms of heat transfer and friction the same boundary conditions were used as in the specimen's upsetting. In each pass the ingot was drawn from the bottom to the top using flat dies of 700 mm width. The manipulator's tong was 'glued' to the bottom end of the workpiece, so that the first bite of each pass had to be set with full dies.
The strain distribution on the centerline of both ingots after the 4th pass is given in Figure 8 for both, the isotropic von Mises and the anisotropic Barlat case. A comparison of the two different yield criteria shows only minor deviations when the total plastic strain ε_t is considered. In this case, the different orientations of the elements coordinate systems do not seem to have a major influence on the deformation calculated for the ingots' central axis. While the total plastic strain

$$\varepsilon_t = \int \dot{\bar{\varepsilon}}^p \, dt \tag{5}$$

is a state variable for the work hardening state of the material and thus strictly increasing during deformation, the equivalent plastic strain

$$\varepsilon_{eq} = \sqrt{\frac{2}{3}\varepsilon_{ij}^p \varepsilon_{ij}^p} \tag{6}$$

measures the geometrical distortion. Due to a possible reversal of direction in plastic flow, this comparative value to the entire plastic deformation is not steadily increasing during deformation (i.e. $\varepsilon_{eq} \leq \varepsilon_t$).

Hence, the differences regarding ε_{eq} between the isotropic case and the anisotropic definition of the two remelting batches represent the effect of the plastic yield's orientation dependency. Generally, the isotropic von Mises definition results in a smoother strain distribution compared to the pronounced variations in the anisotropic Barlat case. The comparison of calculated strain distributions for the two different remelting batches can lead to the conclusion that core fiber deformation increases with pool depth.

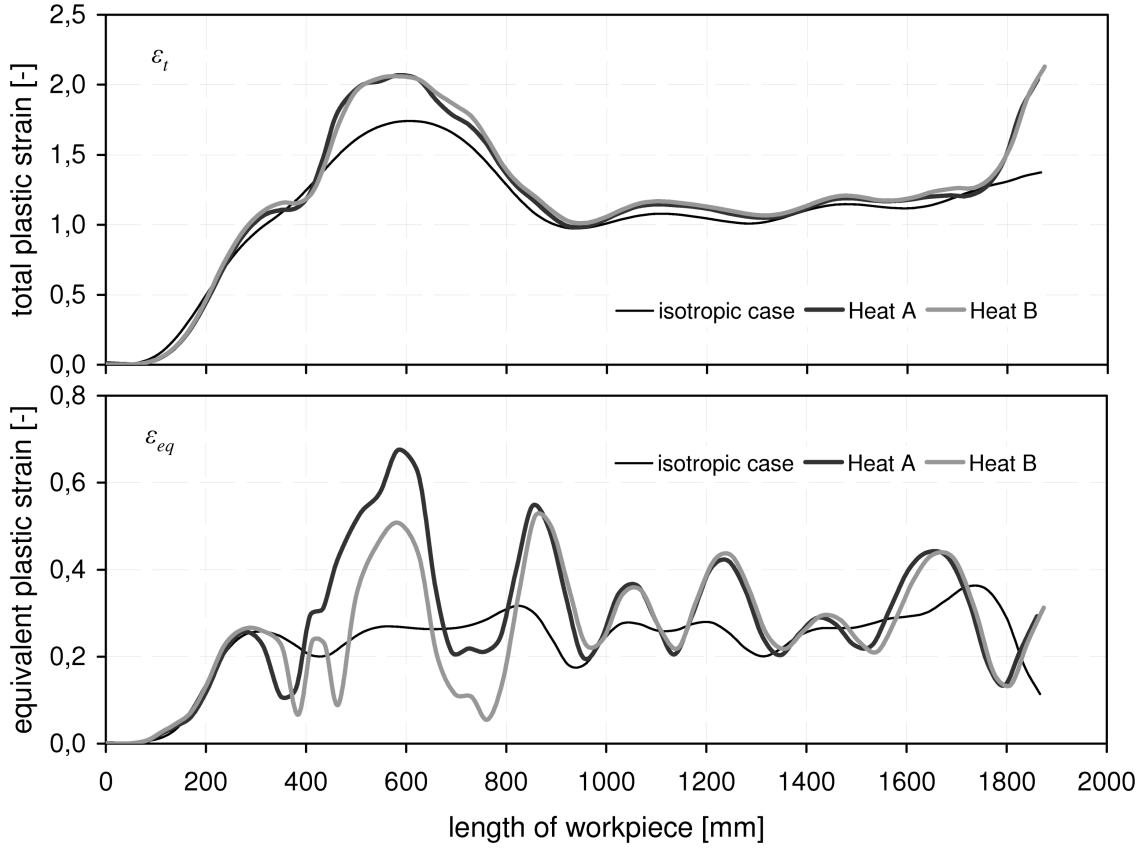

Figure 8. Strain distributions on the core fiber of the ingots after the 4th pass.

The probability of material damage calculated with the normalized and modified Le Roy criterion according to Equation 4b is shown for both ingots and each of the 4 passes in Figure 9.
It is obvious, that VAR heat A appears more susceptible to damage as compared to heat B, since the longer solidification times reduce the critical values of the damage criterion. The critical spots, where the occurrence of damage is predicted to be most likely, are related to the edge of the dies; which is well known and often reported in literature [5,15].
However, by modeling the damage resistance as a function of local solidification time, the center region of the ingots' cross-section becomes more sensitive compared to the surface, where the numerical simulation usually predicts crack initiation. Hence, it was of particular interest to see, what the simulation results would say about the damage behavior inside the ingots. The probability of damage calculated by the two modified damage criteria (Equations 4a and b) is shown in a longitudinal section of both ingots after the 4th pass in Figure 10, where $P_{C\&L}$ and P_{LR} are depicted in form of iso-surfaces.
It can be seen that the prolonged duration of solidification in the center region results in an increased sensitivity to damage initiation. The modified and normalized damage criterion based on Cockcroft & Latham generally seems to over predict damage in contrast to the other one by Le Roy. Nevertheless, both criteria show the same tendencies.

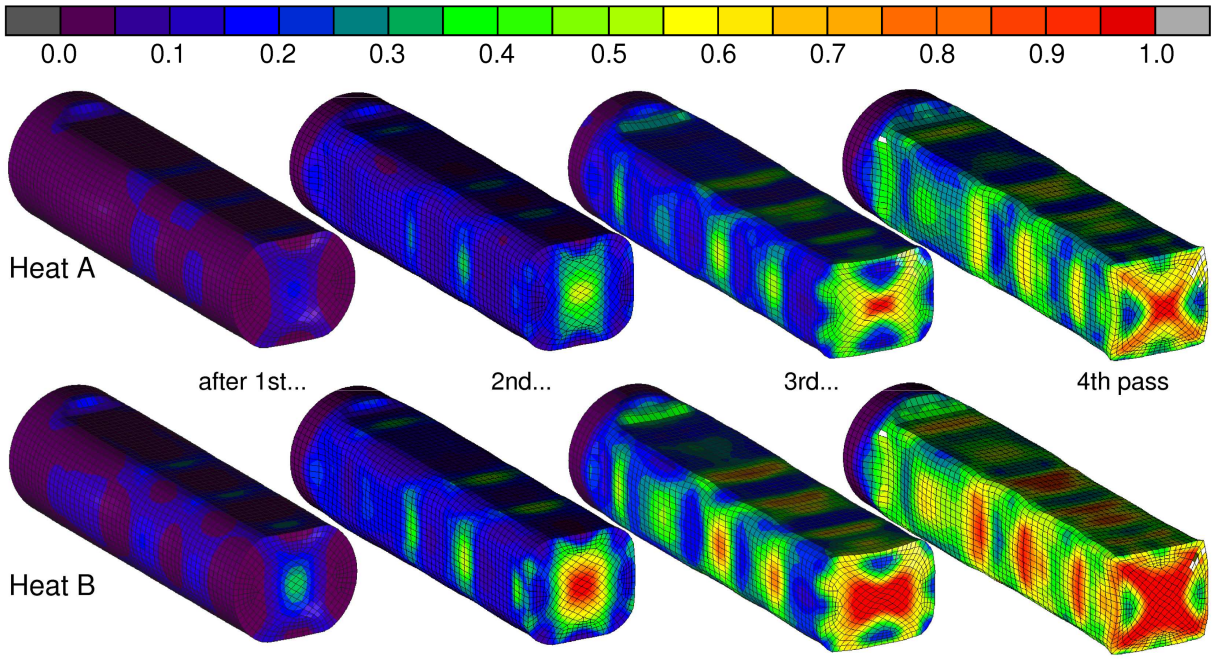

Figure 9. Probability of damage (LR) on the workpieces' surface after all 4 passes.

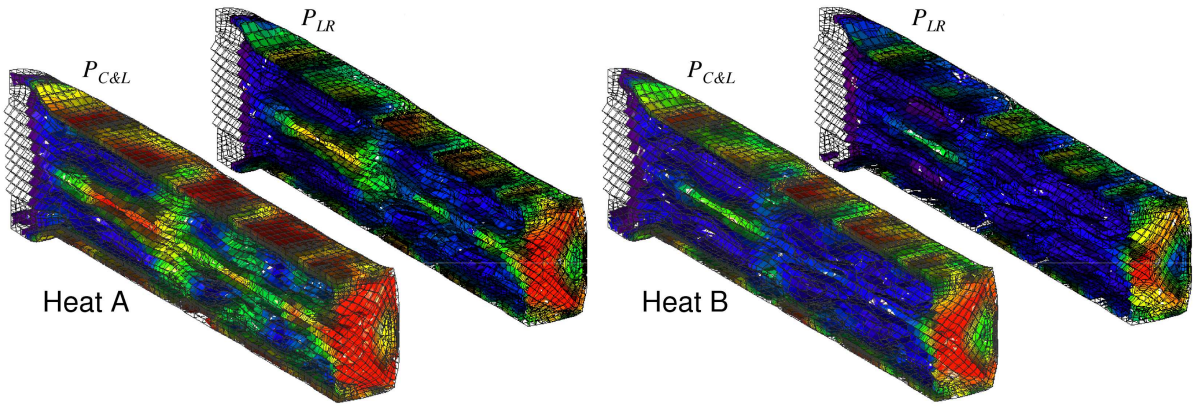

Figure 10. Probability of damage (C&L and LR) inside the workpieces after the 4th pass.

Furthermore, the hypothetically predicted centerline damage is obviously depending on the applied forging practice, especially regarding the choice of bite width. The region of the ingot, in which during all 4 passes the full die width was used, shows a significantly higher probability of damage on the core fiber as the rest of the ingot.

Discussion

In an attempt to close the modeling gap between the subsequent processes of remelting and forging, some properties generated during liquid metal processing and casting were transferred to the initial condition of the material's hot working. In order to determine critical values for selected damage criteria, the commonly used von Mises yield criterion had to be replaced by an anisotropic yield criterion, since remelting results in a distinct texture, which has to be accounted for in the numerical simulation. Barlat's formulation of the material's plastic flow behavior could be expanded to the use under hot working conditions and proved applicable to model the solidification texture developing inside an ingot during VAR.

It is well known, that a material's damage susceptibility during forming depends on its micro-structural state, i.e. grain size, secondary phases, distribution of precipitates etc., which in case of primary hot working operations is determined by the preceding metallurgical processes.
Consequently, in the case of superalloys the material's behavior is directly influenced by process conditions during remelting and the following homogenization treatment. Since the segregation prone superalloys react very sensitive on solidification conditions, the damage resistance was interpreted as a function of local solidification time, which in turn offered the possibility to model a certain inhomogeneity of properties within an ingot. The results of the cogging simulation revealed that with this approach even the classical damage criteria could be used to provoke numerically predicted damage of the ingot's core. Besides the predefined influence of remelting conditions the results of the forming simulation also showed the effect of bite width on damage behavior. However, most damage criteria available in the literature have their origin in cold metal forming applications and therefore do neither account for a temperature dependence nor the influence of microstructural development during hot working. In order to reliably describe material damage in hot working, an appropriate criterion has to include recrystallization, since this enables the material to restore its damage resistance. This would require a new criterion and certainly a large amount of material related input data. As a result, with the currently available damage criteria the numerical simulation can only reveal certain tendencies.

Conclusion

As ingot diameters are increasing, a coupling between solidification conditions and the resulting material properties relevant to its yield behavior is gaining further importance. Since material in the as-cast or coarse-grained homogenized state obviously does not behave as isotropic and homogeneous as the numerical simulation usually assumes, the inhomogeneity of properties within an ingot has to be accounted for in the modeling of a forging process in order to obtain reliable results. An approach to do so was presented. However, not all required material properties can easily be determined and appropriate models to realistically represent real material behavior still need to be developed.

References

1. W. Kurz, D.J. Fisher, *Fundamentals of Solidification* (Trans Tech Publications, 1984), 68-72.

2. H. Hojas, H. Zenner and E. Krainer, "Untersuchungen über den Einfluss der Gussstruktur auf das Verhalten legierter Stähle bei der Warmformgebung", *Archiv für Eisenhüttenwesen* 42 (1971) 9, 603-613.

3. G. Wasle, "COGGING – Physikalische und numerische Simulation der Primärumformung von Nimonic 80a" (Ph.D. Thesis, Technical University Graz, 2003), 69-74.

4. M. Wolske, "Simulation des Werkstoffgefüges beim Schmieden", DFG-Verbundprojekt DT5 (Working Report, RWTH Aachen University, 1999), 58f.

5. S. Riljak, "FEM analysis of open die forging with the application of fracture criteria", *Proc. ESAFORM 5* (2002), 407-410.

6. Y. Dong, Z. Jiang and Z. Li, "Laves Phase Precipitation in Alloy Inconel718 produced by Electroslag Remelting", *Proc. of the 2007 LMPC*, 77-81.

7. X. Liang, R. Zhang, Y. Yang, Y. Han, “An Investigation of the Homogenization and Deformation of Alloy 718 Ingots”, *Superalloys 718, 625, 706 and Various Derivatives* (1994), 947-956.

8. J.M. Poole, K.R. Stultz and J.M. Manning, “The Effect of Ingot Homogenization Practice on the Properties of Wrought Alloy 718 and Structure”, *Superalloy 718 – Metallurgy and Applications* (1989), 219-228.

9. K.C. Mills, *Recommended Values of Thermophysical Properties for selected commercial Alloys* (NPL, ASM International, 2002), 181-190.

10. J. Terhaar, M. Maurischat, N. Blaes D. Bokelmann and K.M. Kelkar, “Calibration of a Simulation Model for VAR with respect to the Influence of Helium Cooling”, *Proc. of the 2009 LMPC*, 13-20.

11. F. Barlat, D.J. Lege, J.C. Brem, “A six-component yield function for anisotropic metals”, *International Journal of Plasticity*, Vol.7 (1991), 693-712.

12. MSC.Software Corporation, *Marc® 2007 r1 – Volume A: Theory and User Information*.

13. M.G. Cockcroft, D.J. Latham, “Ductility and the Workability of Metals”, *Journal of the Institute of Metals*, Vol.96 (1968), 33-39.

14. G. Le Roy, J.D. Embury, G. Edward and M.F. Ashby, “A Model of Ductile Fracture based on the Nucleation and Growth of Voids”, *Acta Metallurgica*, Vol.29 (1981), 1509-1522.

15. M.Wolske, “Umformbarkeit und Modellierung der Gefügeentwicklung von Nickelbasis-legierungen” (Ph.D. Thesis, RWTH Aachen University, 2005), 117f.